

A MATHEMATICAL MODEL TO PREDICT GROWTH AND TREATMENT FOR UPS CANCER

SUMIT ROY

Dedicated to my brother

ABSTRACT. We propose a mathematical model for the growth and treatment dynamics of Undifferentiated Pleomorphic Sarcoma (UPS) based on a system of nonlinear differential equations. The model integrates Gompertz-type tumor growth with surface-area dependent necrotic loss, surgical resection with residual disease, postoperative recovery, tumor-immune interaction, and an optimal radiation treatment component.

We analyze the resulting dynamical system and obtain several properties of the model. The growth equation exhibits a threshold below which tumor volume cannot be sustained. The postoperative phase shows transient dynamics prior to proliferative recovery. For the tumor-immune subsystem, equilibrium states and local stability conditions are identified. The radiation treatment problem is formulated as an optimal control problem, and the optimal strategy is shown to be of bang-bang type.

Numerical simulations illustrate the influence of biological and treatment parameters on tumor evolution, and the results are qualitatively consistent with clinical patterns reported for UPS.

1. INTRODUCTION

This paper presents a mathematical model for studying the growth and treatment dynamics of *Undifferentiated Pleomorphic Sarcoma* (UPS) (see [11]). We describe the basic growth of the tumor using a differential equation. This equation combines a standard Gompertz growth model (see [1], [3]) with a term that accounts for cell death (necrosis) based on the tumor's surface area

$$\frac{dV}{dt} = f(V) = r_g V \ln\left(\frac{K}{V}\right) - \lambda V^{2/3}.$$

In this formula, $V(t)$ is the tumor volume at time t . r_g is how fast the cells multiply, K is the maximum size the body can support, and λ is the rate at which cells die due to lack of nutrients. We prove that if the tumor becomes too small, the death rate becomes higher than the growth rate, and the tumor disappears completely in a short time. Results of this type illustrate how relatively simple growth models can still yield useful mathematical insight into tumor dynamics.

2020 *Mathematics Subject Classification.* 92B05, 92C50, 34H05, 49N90.

Key words and phrases. Undifferentiated Pleomorphic Sarcoma (UPS), Mathematical Oncology, Optimal Control, Hybrid Systems, Tumor-Immune Dynamics, Surgery Modeling.

Address: Stat-Math Unit, Indian Statistical Institute, 203 B.T. Road, Kolkata 700 108, India.

In recent years, mathematical oncology has moved well beyond the use of classical growth laws alone, with increasing attention being given to models that incorporate treatment response, immune effects, and other features of the tumor microenvironment. Recent contributions in the field include broad reviews of tumor growth and treatment-resistance models for solid tumors, roadmaps for current directions in mathematical oncology, and focused studies of cancer immunotherapy from a clinically translatable modeling perspective [12, 13, 14]. These developments show that there is substantial current interest in combining mechanistic tumor growth models with treatment and host-response dynamics in a form that still permits useful mathematical analysis. At the same time, much of the recent literature treats growth, immune interaction, or treatment optimization separately. In the present work, we study a single analytically tractable framework that combines intrinsic tumor growth, surgical resection, postoperative recovery, and treatment timing in the specific setting of UPS, which continues to attract clinical interest because of its aggressive behavior and risk of recurrence [15, 16].

Motivated by these developments, we construct a model that captures several key stages of tumor progression and treatment. Our model is divided into four main parts

- (i) *Surgery Model*: If V is the volume before surgery, the volume after surgery is $\mathcal{R}(V) = (1 - \eta)V + \epsilon$. Here, η is how much of the tumor the surgeon removes, and ϵ is the tiny amount of cancer left behind that cannot be seen (see [10]).
- (ii) *Two-Phase Growth*: After surgery, the tumor goes through two steps. First is the *Inflammatory Phase*. We found a specific formula to solve this

$$V(t) = \left[\left(V_{res}^{1/3} - \frac{\kappa}{r} \right) e^{rt/3} + \frac{\kappa}{r} \right]^3.$$

The second step is the *Proliferative Phase*.

- (iii) *The Switch*: To move from the first phase to the second, we use a switching function $\phi(t)$. This function uses a chemical marker $[c]$ in the body that follows the rule $\frac{dc}{dt} = \beta - \mu c$. This ensures the transition in our model is smooth and realistic.
- (iv) *Radiation Timing*: We use *Pontryagin's Minimum Principle* to find the best time to give radiation. Since the tumor's sensitivity to radiation changes over time ($\Psi(t)$), the best strategy is a bang-bang control (see [9] for details). This means giving the maximum dose (D_{max}) when the tumor is most sensitive

$$D^*(t) = \begin{cases} D_{max} & \text{if } \Psi(t) > \text{threshold} \\ 0 & \text{if } \Psi(t) < \text{threshold.} \end{cases}$$

In addition to these, we also look at the interaction between the tumor (V) and the immune system (E) using the system

$$\begin{aligned}\frac{dV}{dt} &= rV \ln(K/V) - \frac{\delta EV}{m + V} \\ \frac{dE}{dt} &= s + \frac{\rho EV^2}{\eta^2 + V^2} - \mu E.\end{aligned}$$

We use the *Routh-Hurwitz criterion* to prove when the immune system is strong enough to keep the tumor at a stable, small size.

Beyond the formulation of the model, the paper provides several analytical results concerning the resulting dynamical system. In particular, we identify conditions under which the necrosis term induces a minimum viable tumor size, derive explicit solutions for the inflammatory growth phase, and analyze the stability of the tumor-immune equilibrium using the Routh-Hurwitz criterion. Furthermore, we prove that the optimal radiation schedule is of bang-bang type, showing that radiation should be administered at the maximum allowable rate during periods of high radiosensitivity (Theorem 4.4). The present framework therefore provides a unified dynamical systems model for UPS that permits the mathematical analysis of recurrence thresholds, postoperative phase transitions, and treatment timing.

Finally, we compare the qualitative predictions of the model with clinical observations reported for UPS. In the future, we plan to add stochastic equations to the model to account for how every patient is slightly different.

2. TUMOR GROWTH DYNAMICS

Consider the following tumor growth model where proliferation follows Gompertz kinetics and cell loss scales with surface area, i.e.

$$\frac{dV}{dt} = f(V) = \underbrace{r_g V \ln\left(\frac{K}{V}\right)}_{\text{proliferation}} - \underbrace{\lambda V^{2/3}}_{\text{necrosis}}, \quad (2.1)$$

where $V(t)$ represents tumor volume at time t , r_g is the proliferation rate, K is the carrying capacity, and λ is the necrosis coefficient.

Theorem 2.1. *Consider the tumor growth model (2.1) with $\lambda > 0$.*

(i) *If the tumor volume $V(t)$ enters the regime where*

$$r_g V \ln\left(\frac{K}{V}\right) < \lambda V^{2/3},$$

the trajectory $V(t)$ terminates at the boundary $V = 0$ in finite time $t_{ext} < \infty$.

(ii) *For all $V(0) < K$, there exists $\delta > 0$ such that every solution with initial value in $(0, K)$ satisfies*

$$V(t) \leq K - \delta$$

for all sufficiently large t . In particular,

$$\limsup_{t \rightarrow \infty} V(t) < K.$$

Proof. (i) Let

$$g(V) = r_g V^{1/3} \ln \left(\frac{K}{V} \right) - \lambda.$$

Since $\lim_{V \rightarrow 0^+} g(V) = -\lambda$, there exists a $\delta > 0$ such that for all $V \in (0, \delta)$,

$$\frac{dV}{dt} = V^{2/3} g(V) \leq -\frac{\lambda}{2} V^{2/3}.$$

Integrating this inequality gives

$$V(t)^{1/3} \leq V(0)^{1/3} - \frac{\lambda t}{6}.$$

Thus, $V(t)$ must reach zero at some time $t_{ext} \leq \frac{6V(0)^{1/3}}{\lambda}$. The solution is not positive for all t .

(ii) At $V = K$, the growth rate is $f(K) = r_g K \ln(1) - \lambda K^{2/3} = -\lambda K^{2/3} < 0$. By the continuity of $f(V)$, there exists an $\delta > 0$ such that $f(V) < 0$ for all $V \in [K - \delta, K]$. Consequently, once a trajectory enters the interval $[K - \delta, K]$, the vector field points strictly toward smaller values of V . Hence every solution with initial value in $(0, K)$ eventually remains below $K - \delta$, and therefore

$$\limsup_{t \rightarrow \infty} V(t) \leq K - \delta < K.$$

□

Remark 2.1. Part (i) of the above theorem represents the Minimum Viable Volume. Unlike the standard Gompertz model where a single cell ($V \approx 0$) always grows into a tumor, our model suggests that if the initial volume is too small, the metabolic/necrotic costs ($V^{2/3}$) overwhelm the proliferation, leading to successful tumor clearance.

Theorem 2.2. *Let us consider the tumor growth model (2.1) and let V_∞ be the non-trivial stable equilibrium¹. Then the exponential convergence rate α for the linearized system is given by*

$$\alpha = r_g - \frac{1}{3} \lambda V_\infty^{-1/3} = r_g \left[1 - \frac{1}{3} \ln \left(\frac{K}{V_\infty} \right) \right]. \quad (2.2)$$

Proof. The equilibrium V_∞ is defined by the condition $f(V_\infty) = 0$, and for $V_\infty > 0$, this means

$$r_g \ln \left(\frac{K}{V_\infty} \right) = \lambda V_\infty^{-1/3}. \quad (2.3)$$

¹Stability of V_∞ and the positivity of the convergence rate α are guaranteed provided the steady-state volume satisfies $V_\infty > K e^{-3}$, ensuring $1 - \frac{1}{3} \ln(K/V_\infty) > 0$.

We will linearize $f(V)$ to evaluate the stability. Using the product rule on the Gompertz term, we get

$$\begin{aligned} f'(V) &= \frac{d}{dV} \left[r_g V (\ln K - \ln V) - \lambda V^{2/3} \right] \\ &= r_g \left[(\ln K - \ln V) + V \left(-\frac{1}{V} \right) \right] - \frac{2}{3} \lambda V^{-1/3} \\ &= r_g \ln \left(\frac{K}{V} \right) - r_g - \frac{2}{3} \lambda V^{-1/3}. \end{aligned}$$

Therefore at the equilibrium point $V = V_\infty$, we get

$$f'(V_\infty) = r_g \ln \left(\frac{K}{V_\infty} \right) - r_g - \frac{2}{3} \lambda V_\infty^{-1/3}.$$

Thus by substituting the equilibrium identity from (2.3), we obtain

$$\begin{aligned} f'(V_\infty) &= \left(\lambda V_\infty^{-1/3} \right) - r_g - \frac{2}{3} \lambda V_\infty^{-1/3} \\ &= \frac{1}{3} \lambda V_\infty^{-1/3} - r_g. \end{aligned}$$

The local convergence rate α is defined as $-f'(V_\infty)$ to represent the rate of decay of perturbations ($x(t) \sim e^{-\alpha t}$). Thus

$$\alpha = -f'(V_\infty) = r_g - \frac{1}{3} \lambda V_\infty^{-1/3}. \quad (2.4)$$

Again substituting (2.3), we can also express this by

$$\alpha = r_g \left[1 - \frac{1}{3} \ln \left(\frac{K}{V_\infty} \right) \right] \quad (2.5)$$

□

Remark 2.2. The model components describe distinct tumor growth dynamics: the proliferation term $r_g V \ln(K/V)$ captures the transition from quasi-exponential expansion to decelerated growth as the tumor volume V approaches the carrying capacity K , reflecting resource depletion and spatial constraints. The inhibitory term $-\lambda V^{2/3}$ models surface-area dependent effects; specifically, it accounts for nutrient diffusion limitations where the viable proliferating fraction is restricted to the tumor's outer shell, eventually leading to hypoxic core formation in tumors larger than 1 cm³. Table 1 provides characteristic parameters for various malignancies, identifying glioblastoma as having the highest proliferation rate (0.143 day⁻¹), whereas UPS demonstrates aggressive metastatic potential despite intermediate primary growth rates [2, 4, 5, 7, 6].

Figure 1 illustrates the tumor growth trajectories predicted by the modified Gompertz–necrosis model for several tumor types. The trajectories exhibit the typical sigmoidal behavior associated with Gompertzian growth. For small tumor volumes the proliferative term $r_g V \ln(K/V)$ dominates the necrotic loss term $\lambda V^{2/3}$, producing rapid early expansion. As the tumor volume increases, however, the logarithmic slowdown in the Gompertz component

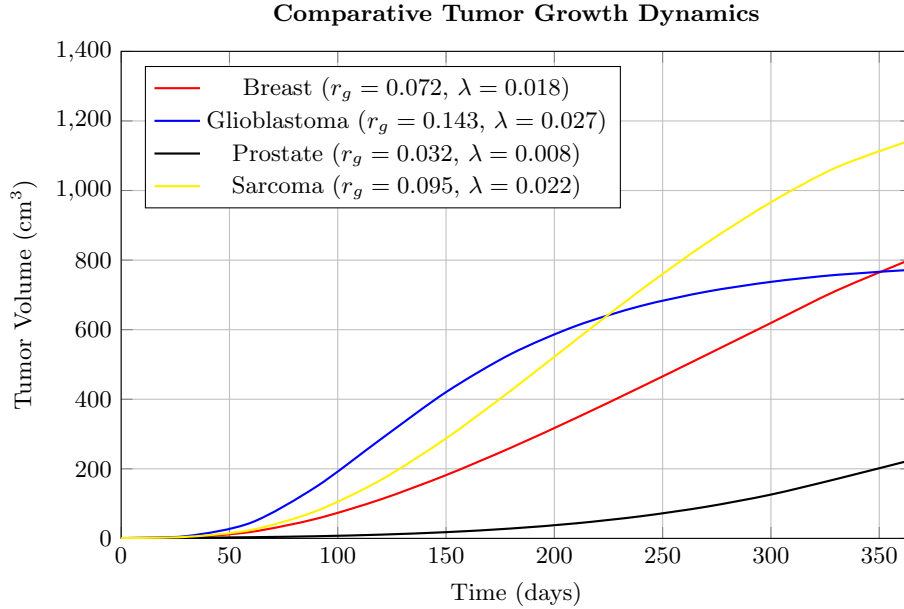


FIGURE 1. Comparison of tumor growth trajectories predicted by the modified Gompertz–necrosis model for representative tumor types.

together with the surface-mediated loss term gradually reduces the net growth rate, causing the curves to bend and approach a slower long-term growth regime.

Differences between the trajectories reflect the biological variability between tumor types. In particular, tumors with larger effective proliferation rates exhibit steeper early growth, while those with stronger inhibitory effects display more gradual progression. The UPS trajectory lies among the more aggressive profiles over the time interval considered, which is consistent with the clinically reported rapid progression of this tumor type.

TABLE 1. Tumor growth parameters

Tumor Type	r_g (day ⁻¹)	λ (day ⁻¹)	K (cm ³)
Breast	0.072	0.018	1200
Glioblastoma	0.143	0.027	800
Prostate	0.032	0.008	1500
Sarcoma	0.095	0.022	2500
UPS	0.108	0.026	1800

Table 1 lists the parameter values used in the growth simulations. The parameter r_g represents the intrinsic proliferation rate of tumor cells, while λ models cell loss due to necrosis and nutrient limitations near the tumor surface. The carrying capacity K reflects environmental constraints on the maximum tumor volume that can be sustained. Variations

in these parameters allow the model to reproduce the different growth patterns observed across tumor types while preserving the same underlying dynamical structure.

3. SURGICAL RESECTION MODULE

3.1. Mathematical Formulation and Analysis. Let $\Omega = \{V \in \mathbb{R} : 0 < V < K\}$ denote the biologically relevant range of positive tumor volumes. In the postoperative analysis below, we restrict attention to trajectories that remain in the positive regime and evolve in a neighborhood of the positive postoperative equilibrium.

Theorem 3.1. *Let the postoperative tumor volume $V(t)$ be governed by the non-linear system*

$$\frac{dV}{dt} = f_p(V) = r_p V \ln \left(\frac{K_{post}}{V} \right) - \lambda V^{2/3}, \quad V(t_{op}^+) = V_{res} \quad (3.1)$$

where $r_p, K_{post}, \lambda > 0$. Assume that the postoperative system admits a positive equilibrium $V_{\infty,p} \in (0, K_{post})$ satisfying

$$r_p \ln \left(\frac{K_{post}}{V_{\infty,p}} \right) = \lambda V_{\infty,p}^{-1/3}.$$

The dynamics satisfy

- (i) The equilibrium $V_{\infty,p}$ is locally asymptotically stable provided $V_{\infty,p} > K_{post}e^{-3}$.
- (ii) The local convergence rate α_p is given by:

$$\alpha_p = r_p \left(1 - \frac{1}{3} \ln \left(\frac{K_{post}}{V_{\infty,p}} \right) \right). \quad (3.2)$$

- (iii) For trajectories starting sufficiently close to $V_{\infty,p}$, the linearized dynamics satisfy

$$|x(t)| = |x(t_{op})|e^{-\alpha_p(t-t_{op})}, \quad x(t) = V(t) - V_{\infty,p}.$$

In particular, the nonlinear system exhibits local exponential decay toward $V_{\infty,p}$.

Proof. For the local stability, we linearize $f_p(V)$ about the steady state $V_{\infty,p}$. Let $x(t) = V(t) - V_{\infty,p}$ denote a small perturbation. Then the first-order expansion gives $\frac{dx}{dt} = f'_p(V_{\infty,p})x$. Therefore

$$\begin{aligned} f'_p(V) &= \frac{d}{dV} \left[r_p V (\ln K_{post} - \ln V) - \lambda V^{2/3} \right] \\ &= r_p \ln \left(\frac{K_{post}}{V} \right) - r_p - \frac{2}{3} \lambda V^{-1/3} \end{aligned}$$

At the steady state $V_{\infty,p}$, by substitute the equilibrium identity $\lambda V_{\infty,p}^{-1/3} = r_p \ln\left(\frac{K_{\text{post}}}{V_{\infty,p}}\right)$, we obtain

$$\begin{aligned} f'_p(V_{\infty,p}) &= r_p \ln\left(\frac{K_{\text{post}}}{V_{\infty,p}}\right) - r_p - \frac{2}{3} \left(r_p \ln\left(\frac{K_{\text{post}}}{V_{\infty,p}}\right) \right) \\ &= \frac{1}{3} r_p \ln\left(\frac{K_{\text{post}}}{V_{\infty,p}}\right) - r_p \\ &= -r_p \left(1 - \frac{1}{3} \ln\left(\frac{K_{\text{post}}}{V_{\infty,p}}\right) \right) \end{aligned}$$

By defining $\alpha_p = -f'_p(V_{\infty,p})$, we observe that $\alpha_p > 0$ for $V_{\infty,p} > K_{\text{post}}e^{-3}$. According to the Hartman-Grobman Theorem, the linearized dynamics $\frac{dx}{dt} = -\alpha_p x$ characterize the local stability. This gives (i) and (ii).

For part (iii), let

$$x(t) = V(t) - V_{\infty,p}$$

denote the deviation from the equilibrium. Since $V_{\infty,p}$ is an equilibrium of the postoperative growth equation

$$\frac{dV}{dt} = f_p(V),$$

we have

$$f_p(V_{\infty,p}) = 0.$$

Expanding $f_p(V)$ about $V_{\infty,p}$, we obtain

$$f_p(V) = f_p(V_{\infty,p}) + f'_p(V_{\infty,p})(V - V_{\infty,p}) + \mathcal{O}((V - V_{\infty,p})^2).$$

Therefore

$$\dot{x}(t) = f'_p(V_{\infty,p})x(t) + \mathcal{O}(x(t)^2).$$

Neglecting the higher-order term gives the linearized equation

$$\dot{x}(t) = f'_p(V_{\infty,p})x(t).$$

From part (ii), we have

$$\alpha_p = -f'_p(V_{\infty,p}) > 0,$$

so the linearized system may be written as

$$\dot{x}(t) = -\alpha_p x(t).$$

This is a first-order linear equation, and its solution with initial condition $x(t_{op}) = V_{\text{res}} - V_{\infty,p}$ is

$$x(t) = x(t_{op})e^{-\alpha_p(t-t_{op})}.$$

Hence

$$|x(t)| = |x(t_{op})|e^{-\alpha_p(t-t_{op})}.$$

This proves the exponential decay for the linearized dynamics. Since f_p is continuously differentiable near $V_{\infty,p}$ and $f'_p(V_{\infty,p}) < 0$, standard linearization theory implies that the

equilibrium $V_{\infty,p}$ is locally exponentially stable for the nonlinear system as well. Thus, for initial conditions sufficiently close to $V_{\infty,p}$, the nonlinear trajectory converges exponentially to $V_{\infty,p}$. \square

Theorem 3.2. *Let $\mathcal{R} : \mathbb{R}^+ \rightarrow \mathbb{R}^+$ be the surgical operator defined by*

$$\mathcal{R}(V) = (1 - \eta)V + \epsilon,$$

where $\eta \in (0, 1)$ is the resection efficiency and $\epsilon > 0$ is the minimum residual volume. Then

- (i) \mathcal{R} has a unique fixed point at $V^* = \epsilon/\eta$, representing the volume invariant under the operator's action.
- (ii) \mathcal{R} is a global contraction on $(0, \infty)$ with Lipschitz constant $L = 1 - \eta$.
- (iii) For any $V > 0$, $\mathcal{R}(V) \geq \epsilon$, ensuring the presence of residual disease post-intervention.

Proof. (i) Suppose V^* is a fixed point of \mathcal{R} , i.e. $\mathcal{R}(V^*) = V^*$. Then

$$\begin{aligned} (1 - \eta)V^* + \epsilon &= V^* \\ \Rightarrow \eta V^* &= \epsilon \\ \Rightarrow V^* &= \epsilon/\eta. \end{aligned}$$

Since $\eta \neq 0$, the point $V^* = \epsilon/\eta$ is unique.

(ii) For any $V_1, V_2 \in \mathbb{R}^+$, the Euclidean distance between images $\mathcal{R}(V_1)$ and $\mathcal{R}(V_2)$ is given by

$$\begin{aligned} d(\mathcal{R}(V_1), \mathcal{R}(V_2)) &= |(1 - \eta)V_1 + \epsilon - (1 - \eta)V_2 - \epsilon| \\ &= (1 - \eta)|V_1 - V_2|. \end{aligned}$$

Given $\eta \in (0, 1)$, it follows that $0 < 1 - \eta < 1$, satisfying the definition of a contraction mapping with the Lipschitz constant $L = 1 - \eta$.

(iii) Since $V > 0$ and $(1 - \eta) \geq 0$, their product $(1 - \eta)V$ is non-negative. Therefore,

$$\mathcal{R}(V) = (1 - \eta)V + \epsilon \geq \epsilon.$$

This precludes total eradication ($V = 0$) in a single application of the operator. \square

The parameters listed in this table describe the surgical resection stage of the model. The parameter η represents the fraction of tumor mass removed during surgery, while ϵ denotes the residual microscopic tumor burden that cannot be completely eliminated. The operator

$$\mathcal{R}(V) = (1 - \eta)V + \epsilon$$

therefore produces an immediate reduction in tumor volume followed by a small residual population that can subsequently regrow. This captures the clinically observed phenomenon that even successful resection may leave microscopic disease capable of initiating tumor recurrence.

TABLE 2. Standard UPS Resection Parameters

Parameter	Description	Value
V_0	Initial volume	120 cm ³
η	Resection efficiency	0.85
ϵ	Residual volume	0.8 cm ³
r_g	Pre-op growth rate	0.15 day ⁻¹
r_p	Post-op growth rate	0.10 day ⁻¹
K	Carrying capacity	500 cm ³
K_{post}	Post-op capacity	300 cm ³

Proposition 1. *Let $\mathcal{R}(V)$ be the resection operator with fixed point $V^* = \epsilon/\eta$. The immediate impact of the intervention depends on the ratio*

$$\zeta := \frac{\eta V(t_{op}^-)}{\epsilon}$$

between the intended reduction and the residual constant. Then

- (i) *If $\zeta > 1$ then the preoperative volume exceeds the operator's fixed point, i.e. $V(t_{op}^-) > V^*$, and the intervention successfully reduces the tumor volume, i.e. $V_{res} < V(t_{op}^-)$, though it remains bounded below by V^* .*
- (ii) *If $\zeta = 1$, then the preoperative volume equals the fixed point, i.e. $(V(t_{op}^-) = V^*)$, and resulting in no net change in volume post-intervention, i.e. $V_{res} = V^*$.*
- (iii) *If $\zeta < 1$ then the preoperative volume is below the fixed point, i.e. $V(t_{op}^-) < V^*$, and the intervention results in an increase in measurable residual volume, i.e. $V_{res} > V(t_{op}^-)$ due to the dominance of the residual constant ϵ .*

Proof. The postoperative volume is given by

$$V_{res} = \mathcal{R}(V(t_{op}^-)) = (1 - \eta)V(t_{op}^-) + \epsilon.$$

Now by putting $\epsilon = \eta V^*$, we get

$$V_{res} = (1 - \eta)V(t_{op}^-) + \eta V^*.$$

Then by subtracting $V(t_{op}^-)$ from both sides, we get

$$\Delta V := V_{res} - V(t_{op}^-) = -\eta V(t_{op}^-) + \eta V^* = \eta(V^* - V(t_{op}^-)).$$

The sign of the change depends entirely on the relation between $V(t_{op}^-)$ and V^* , i.e.

- (i) *If $\zeta > 1$, then $V(t_{op}^-) > V^*$, implying $\Delta V < 0$. So the size of the tumor reduces.*
- (ii) *If $\zeta = 1$, then $V(t_{op}^-) = V^*$, implying $\Delta V = 0$. So no change in the tumor size.*
- (iii) *If $\zeta < 1$, then $V(t_{op}^-) < V^*$, implying $\Delta V > 0$. So the size of the tumor increases.*

Furthermore, the distance to the fixed point is

$$V_{res} - V^* = (1 - \eta)(V(t_{op}^-) - V^*).$$

Since $|1 - \eta| < 1$, the operator is a contraction, mapping all initial volumes toward V^* over repeated applications. \square

3.2. Therapeutic Implications.

Proposition 2. *To prevent clinical recurrence and maintain the tumor volume below a critical threshold $V(t) \leq V_{crit}$ as $t \rightarrow \infty$, the adjuvant therapy's effective kill rate δ must satisfy*

$$\delta \geq r_p \ln \left(\frac{K_{post}}{V_{crit}} \right) - \lambda V_{crit}^{-1/3} \quad (3.3)$$

Using UPS parameters ($r_p = 0.10, K_{post} = 300, \lambda = 0.05$), this requires $\delta \geq 0.23 \text{ day}^{-1}$ for $V_{crit} = 24.6$.

Proof. The postoperative dynamics under continuous adjuvant intervention are described by the augmented system

$$\frac{dV}{dt} = f_p(V) - \delta V = r_p V \ln \left(\frac{K_{post}}{V} \right) - \lambda V^{2/3} - \delta V$$

For the tumor to remain stable or regress at the recurrence threshold V_{crit} , we require the growth rate to be non-positive, i.e.

$$\begin{aligned} & \left. \frac{dV}{dt} \right|_{V_{crit}} \leq 0 \\ \Rightarrow & r_p V_{crit} \ln \left(\frac{K_{post}}{V_{crit}} \right) - \lambda V_{crit}^{2/3} - \delta V_{crit} \leq 0 \\ \Rightarrow & r_p \ln \left(\frac{K_{post}}{V_{crit}} \right) - \lambda V_{crit}^{-1/3} - \delta \leq 0 \quad (\text{as } V_{crit} > 0) \\ \Rightarrow & \delta \geq r_p \ln \left(\frac{K_{post}}{V_{crit}} \right) - \lambda V_{crit}^{-1/3} \end{aligned}$$

\square

Corollary 3.2.1. *The maximum allowable delay between the surgical event at t_{op} and the initiation of adjuvant therapy at t_{int} to ensure the tumor volume does not exceed a secondary safety limit V_{limit} is given by*

$$\Delta t = t_{int} - t_{op} < \frac{1}{r_p} \ln \left(\frac{\ln(K_{post}/V_{res})}{\ln(K_{post}/V_{limit})} \right) \quad (3.4)$$

where $V_{res} = (1 - \eta)V(t_{op}^-) + \epsilon$. In particular, for $V_{limit} = 150 \text{ cm}^3$ and $V_{res} = 25 \text{ cm}^3$, the window is $\Delta t \approx 10.3$ days.

Proof. The postoperative tumor dynamics during the untreated period $t \in [t_{op}, t_{int}]$ are governed by

$$\frac{dV}{dt} = r_p V \ln \left(\frac{K_{post}}{V} \right) - \lambda V^{2/3}. \quad (3.5)$$

Thus,

$$dt = \frac{dV}{r_p V \ln\left(\frac{K_{\text{post}}}{V}\right) - \lambda V^{2/3}}$$

Integrating both sides from the surgical state (t_{op}, V_{res}) to the intervention state $(t_{\text{int}}, V_{\text{limit}})$, we get

$$\int_{t_{op}}^{t_{\text{int}}} d\tau = \int_{V_{\text{res}}}^{V_{\text{limit}}} \frac{dV}{r_p V \ln\left(\frac{K_{\text{post}}}{V}\right) - \lambda V^{2/3}}. \quad (3.6)$$

As $\lambda V^{2/3}$ acts as an inhibitory term, we observe that for any $V > 0$:

$$r_p V \ln\left(\frac{K_{\text{post}}}{V}\right) - \lambda V^{2/3} < r_p V \ln\left(\frac{K_{\text{post}}}{V}\right).$$

Thus, by neglecting the metabolic term $-\lambda V^{2/3}$, we obtain a conservative upper bound for the growth rate. This simplification allows for the analytical solution of the integral

$$\Delta t \approx \int_{V_{\text{res}}}^{V_{\text{limit}}} \frac{dV}{r_p V \ln\left(\frac{K_{\text{post}}}{V}\right)}.$$

Let $u = \ln(K_{\text{post}}/V)$, then $du = -\frac{1}{V}dV$. Therefore, by substituting these into the integral, we get

$$\Delta t \approx -\frac{1}{r_p} \int_{\ln(K_{\text{post}}/V_{\text{res}})}^{\ln(K_{\text{post}}/V_{\text{limit}})} \frac{du}{u}.$$

Thus,

$$\Delta t \approx -\frac{1}{r_p} [\ln |u|]_{\ln(K_{\text{post}}/V_{\text{res}})}^{\ln(K_{\text{post}}/V_{\text{limit}})} = -\frac{1}{r_p} \left[\ln\left(\ln \frac{K_{\text{post}}}{V_{\text{limit}}}\right) - \ln\left(\ln \frac{K_{\text{post}}}{V_{\text{res}}}\right) \right]$$

Hence,

$$t_{\text{int}} - t_{op} = \frac{1}{r_p} \ln \left[\frac{\ln(K_{\text{post}}/V_{\text{res}})}{\ln(K_{\text{post}}/V_{\text{limit}})} \right] \quad (3.7)$$

Since the term $-\lambda V^{2/3}$ reduces the growth rate, the expression above should be interpreted as a conservative analytical estimate for the allowable delay before intervention. \square

4. POSTOPERATIVE RECOVERY DYNAMICS IN UPS

4.1. Inflammatory Phase Model. The postoperative inflammatory phase follows the dynamics

$$\frac{dV}{dt} = (r_{\text{inflam}} - \delta_{\text{immune}})V - \kappa_{\text{hypoxia}}V^{2/3}, \quad (4.1)$$

where r_{inflam} is the intrinsic proliferation rate stimulated by postoperative inflammatory cytokines, δ_{immune} is the rate of tumor cell clearance by the recruited innate immune response, and κ_{hypoxia} is the hypoxic stress coefficient representing metabolic cell death due to vascular disruption. Let the net effective growth rate be $r = r_{\text{inflam}} - \delta_{\text{immune}}$.

Theorem 4.1. *For $r \neq 0$, the above system (4.1) admits the analytical solution*

$$V(t) = \left[\left(V_{\text{res}}^{1/3} - \frac{\kappa_{\text{hypoxia}}}{r} \right) e^{rt/3} + \frac{\kappa_{\text{hypoxia}}}{r} \right]^3 \quad (4.2)$$

where V_{res} is the volume immediately following surgery. The qualitative behavior is determined by r . In particular,

- (i) If immune clearance dominates, i.e. $r < 0$, then $V(t)$ is strictly monotonically decreasing and converges to $V = 0$ in finite time

$$T_{ext} = \frac{3}{|r|} \ln \left(1 + \frac{|r|V_{res}^{1/3}}{\kappa_{hypoxia}} \right) \quad (4.3)$$

- (ii) If $r > 0$, then there exists an unstable equilibrium (threshold) at

$$V_{threshold} = \left(\frac{\kappa_{hypoxia}}{r} \right)^3,$$

and if $V_{res} < V_{threshold}$, the hypoxic term dominates, leading to regression despite a positive net growth rate.

Proof. We will use the Bernoulli-type transformation $W = V^{1/3}$ to solve the equation

$$\frac{dV}{dt} = rV - \kappa_{hypoxia}V^{2/3}.$$

Now $W = V^{1/3}$ gives

$$\frac{dW}{dt} = \frac{1}{3}V^{-2/3}\frac{dV}{dt}.$$

Then

$$\frac{dW}{dt} = \frac{1}{3}V^{-2/3} \left[rV - \kappa_{hypoxia}V^{2/3} \right] = \frac{r}{3}W - \frac{\kappa_{hypoxia}}{3}.$$

This gives a first-order linear non-homogeneous equation, and to solve this we use the integrating factor $\mu(t) = e^{-\int(r/3)dt} = e^{-rt/3}$. This gives

$$\frac{d}{dt} \left(W e^{-rt/3} \right) = -\frac{\kappa_{hypoxia}}{3} e^{-rt/3}$$

Integrating both sides from 0 to t gives

$$\begin{aligned} W(t)e^{-rt/3} - W(0) &= \int_0^t -\frac{\kappa_{hypoxia}}{3} e^{-r\tau/3} d\tau \\ \Rightarrow W(t)e^{-rt/3} - V_{res}^{1/3} &= \left[\frac{\kappa_{hypoxia}}{r} e^{-r\tau/3} \right]_0^t \\ \Rightarrow W(t)e^{-rt/3} &= V_{res}^{1/3} + \frac{\kappa_{hypoxia}}{r} \left(e^{-rt/3} - 1 \right). \end{aligned}$$

Multiplying through by $e^{rt/3}$ and rearranging terms, we get

$$W(t) = \left(V_{res}^{1/3} - \frac{\kappa_{hypoxia}}{r} \right) e^{rt/3} + \frac{\kappa_{hypoxia}}{r}.$$

Thus,

$$V(t) = \left[\left(V_{res}^{1/3} - \frac{\kappa_{hypoxia}}{r} \right) e^{rt/3} + \frac{\kappa_{hypoxia}}{r} \right]^3$$

For $r < 0$, let $r = -|r|$. Extinction occurs when $W(T_{ext}) = 0$. So,

$$0 = \left(V_{res}^{1/3} - \frac{\kappa_{hypoxia}}{-|r|} \right) e^{-|r|T_{ext}/3} + \frac{\kappa_{hypoxia}}{-|r|}.$$

Rearranging terms, we get

$$\frac{\kappa_{\text{hypoxia}}}{|r|} = \left(V_{\text{res}}^{1/3} + \frac{\kappa_{\text{hypoxia}}}{|r|} \right) e^{-|r|T_{\text{ext}}/3}.$$

Thus

$$e^{|r|T_{\text{ext}}/3} = \frac{V_{\text{res}}^{1/3} + \frac{\kappa_{\text{hypoxia}}}{|r|}}{\frac{\kappa_{\text{hypoxia}}}{|r|}} = \frac{|r|V_{\text{res}}^{1/3}}{\kappa_{\text{hypoxia}}} + 1.$$

Therefore,

$$\begin{aligned} \frac{|r|T_{\text{ext}}}{3} &= \ln \left(1 + \frac{|r|V_{\text{res}}^{1/3}}{\kappa_{\text{hypoxia}}} \right) \\ \Rightarrow T_{\text{ext}} &= \frac{3}{|r|} \ln \left(1 + \frac{|r|V_{\text{res}}^{1/3}}{\kappa_{\text{hypoxia}}} \right). \end{aligned}$$

This completes the proof. \square

4.2. Proliferative Phase Analysis.

Theorem 4.2. *Consider the tumor volume dynamics on the interval $\Omega = (0, K)$ defined by*

$$\frac{dV}{dt} = r_p V \left(1 - \frac{V}{K} \right) - \gamma V^{3/4} + \eta V^{1/2} = G(V). \quad (4.4)$$

The terms $-\gamma V^{3/4}$ and $\eta V^{1/2}$ are used here as phenomenological corrections representing, respectively, inhibitory stress effects and residual recovery-driven growth during the postoperative proliferative phase.

Assume that $G(K) < 0$. Then there exists at least one equilibrium $V_c \in (0, K)$. Moreover, if an equilibrium $V_c \in (0, K)$ satisfies $G'(V_c) < 0$, then V_c is locally exponentially stable. In that case, the linearized deviation $x(t) = V(t) - V_c$ satisfies

$$|x(t)| \approx |x(0)|e^{-\alpha t}, \quad \alpha = -G'(V_c),$$

and

$$\alpha = \frac{r_p V_c}{K} + \frac{1}{4} \gamma V_c^{-1/4} + \frac{1}{2} r_p \left(1 - \frac{V_c}{K} \right).$$

Proof. Since

$$G(V) = r_p V \left(1 - \frac{V}{K} \right) - \gamma V^{3/4} + \eta V^{1/2},$$

we have

$$\lim_{V \rightarrow 0^+} G(V) = 0^+,$$

because the positive term $\eta V^{1/2}$ dominates the negative term $\gamma V^{3/4}$ near $V = 0$. On the other hand, by assumption,

$$G(K) < 0.$$

Hence, by continuity, there exists at least one equilibrium $V_c \in (0, K)$ such that $G(V_c) = 0$.

To analyze local stability, we compute

$$G'(V) = r_p \left(1 - \frac{2V}{K}\right) - \frac{3}{4}\gamma V^{-1/4} + \frac{1}{2}\eta V^{-1/2}.$$

If $G'(V_c) < 0$, then the linearized equation

$$\dot{x} = G'(V_c)x$$

has exponentially decaying solutions, and therefore V_c is locally exponentially stable.

Using the equilibrium identity

$$r_p \left(1 - \frac{V_c}{K}\right) - \gamma V_c^{-1/4} + \eta V_c^{-1/2} = 0,$$

we may rewrite $G'(V_c)$ as

$$G'(V_c) = -\frac{r_p V_c}{K} - \frac{1}{4}\gamma V_c^{-1/4} - \frac{1}{2}r_p \left(1 - \frac{V_c}{K}\right).$$

Thus

$$\alpha = -G'(V_c) = \frac{r_p V_c}{K} + \frac{1}{4}\gamma V_c^{-1/4} + \frac{1}{2}r_p \left(1 - \frac{V_c}{K}\right),$$

which proves the stated expression for the local decay rate. \square

4.3. Phase Transition Analysis.

Theorem 4.3. *The global system dynamics transition from the inflammatory growth rate $G_{inf}(V)$ to the proliferative growth rate $G_{pro}(V)$ via a composite switching function $\phi(t) \in [0, 1]$, i.e.*

$$\frac{dV}{dt} = [1 - \phi(t)]G_{inf}(V) + \phi(t)G_{pro}(V). \quad (4.5)$$

Here the switching function is defined as

$$\phi(t) = \left(\frac{[IL - 6](t)^n}{[IL - 6](t)^n + \theta^n} \right) \left(\frac{1}{1 + e^{-k(t-t_0)}} \right), \quad (4.6)$$

where $[IL - 6](t)$ follows the first-order kinetics $\frac{d}{dt}[IL - 6] = \beta - \mu[IL - 6]$. The transition exhibits a temporal width Δt , defined as the interval where the temporal component shifts from 10% to 90% of its saturation value, given by

$$\Delta t = \frac{2 \ln(9)}{k} \approx \frac{4.394}{k} \quad (4.7)$$

Here $IL - 6$ is used as a phenomenological marker of postoperative inflammatory activity, and the switching function is intended to represent the gradual transition from inflammation-dominated dynamics to proliferative recovery.

Proof. The switching function $\phi(t)$ is the product of a biochemical trigger (Hill function) and a temporal smoothing term (Logistic function). First, we solve the kinetics for the biomarker $c(t) = [IL - 6](t)$ using

$$\frac{dc}{dt} + \mu c = \beta.$$

Using the integrating factor $e^{\mu t}$, the general solution is given by

$$c(t) = \frac{\beta}{\mu} + \left(c_0 - \frac{\beta}{\mu} \right) e^{-\mu t}$$

As $t \rightarrow \infty$, $c(t)$ approaches the steady-state β/μ . The Hill component $\frac{c^n}{c^n + \theta^n}$ ensures that the transition is biologically gated by the concentration $c(t)$ crossing the threshold θ .

Next, we derive the temporal width Δt of the logistic term $S(t) = \frac{1}{1 + e^{-k(t-t_0)}}$. We define t_{10} and t_{90} as the time points where $S(t)$ reaches 0.1 and 0.9 respectively,

$$\begin{aligned} \frac{1}{1 + e^{-k(t_{10}-t_0)}} &= 0.1 \\ \Rightarrow 1 + e^{-k(t_{10}-t_0)} &= 10 \\ \Rightarrow e^{-k(t_{10}-t_0)} &= 9 \\ \Rightarrow -k(t_{10} - t_0) &= \ln(9) \\ \Rightarrow t_{10} &= t_0 - \frac{\ln 9}{k}. \end{aligned}$$

Similarly, for the 90% point,

$$\begin{aligned} \frac{1}{1 + e^{-k(t_{90}-t_0)}} &= 0.9 \\ \Rightarrow 1 + e^{-k(t_{90}-t_0)} &= \frac{10}{9} \\ \Rightarrow e^{-k(t_{90}-t_0)} &= \frac{1}{9} \\ \Rightarrow -k(t_{90} - t_0) &= \ln(1/9) = -\ln(9) \\ \Rightarrow t_{90} &= t_0 + \frac{\ln 9}{k}. \end{aligned}$$

The transition width is calculated as:

$$\Delta t = t_{90} - t_{10} = \left(t_0 + \frac{\ln 9}{k} \right) - \left(t_0 - \frac{\ln 9}{k} \right) = \frac{2 \ln 9}{k}$$

Since $\phi(t)$ is a product of differentiable functions, the resulting growth rate $\frac{dV}{dt}$ remains continuous and differentiable, which ensures numerical stability in the hybrid model. \square

4.4. Optimal Radiation Timing. Radiation therapy is typically administered under clinical constraints on both the instantaneous dose rate and the total amount of radiation that can be delivered during a treatment window. In the present model, the effect of radiation on the tumor volume is described by the decay equation

$$\frac{dV}{dt} = -\Psi(t)D(t)V,$$

where $\Psi(t)$ represents the time-dependent radiosensitivity of the tumor and $D(t)$ denotes the radiation dose rate. The radiosensitivity is assumed to vary periodically,

$$\Psi(t) = \alpha + \beta \sin\left(\frac{2\pi t}{\tau}\right),$$

reflecting biological fluctuations in tumor response to radiation.

We assume that the admissible dose schedules satisfy the bounds

$$0 \leq D(t) \leq D_{\max},$$

together with a total dose constraint

$$\int_0^T D(t) dt \leq D_{\text{total}}.$$

The goal is to determine a radiation schedule that minimizes the terminal tumor volume $V(T)$.

Theorem 4.4. *Consider the radiation-induced volume decay*

$$\frac{dV}{dt} = -\Psi(t)D(t)V,$$

where

$$\Psi(t) = \alpha + \beta \sin\left(\frac{2\pi t}{\tau}\right)$$

denotes the time-dependent radiosensitivity and assume $\Psi(t) \geq 0$ for $t \in [0, T]$.

Let the admissible dose schedules satisfy

$$0 \leq D(t) \leq D_{\max}, \quad \int_0^T D(t) dt \leq D_{\text{total}}.$$

Then any dose schedule $D^*(t)$ minimizing the terminal tumor volume $V(T)$ is of bang-bang type. More precisely, there exists a constant threshold λ such that

$$D^*(t) = \begin{cases} D_{\max}, & \text{if } \Psi(t) > \lambda, \\ 0, & \text{if } \Psi(t) < \lambda, \end{cases}$$

for almost every $t \in [0, T]$. On the set where $\Psi(t) = \lambda$, the control may take intermediate values so that the total dose constraint is satisfied.

Proof. For any admissible control $D(t)$, the state equation can be solved explicitly. Integrating the equation gives

$$V(T) = V(0) \exp\left(-\int_0^T \Psi(t)D(t) dt\right).$$

Since $V(0)$ is fixed and the exponential function is strictly decreasing in its exponent, minimizing the terminal tumor volume $V(T)$ is equivalent to maximizing the functional

$$J(D) = \int_0^T \Psi(t)D(t) dt$$

over all admissible controls.

Suppose that $D^*(t)$ is an optimal control. We show that the radiation dose must be concentrated at times where the radiosensitivity $\Psi(t)$ is largest. Assume that there exist measurable sets $A, B \subset [0, T]$ of positive measure such that

$$\Psi(t) > \Psi(s) \quad \text{for all } t \in A, s \in B,$$

and

$$D^*(t) < D_{\max} \quad \text{for } t \in A, \quad D^*(s) > 0 \quad \text{for } s \in B.$$

Choose $\varepsilon > 0$ sufficiently small so that the modified control

$$\tilde{D}(t) = \begin{cases} D^*(t) + \varepsilon, & t \in A, \\ D^*(t) - \varepsilon, & t \in B, \\ D^*(t), & \text{otherwise,} \end{cases}$$

remains admissible. By choosing the sets A and B with equal measure, the total dose constraint is preserved.

The corresponding change in the objective functional is

$$J(\tilde{D}) - J(D^*) = \varepsilon \left(\int_A \Psi(t) dt - \int_B \Psi(t) dt \right).$$

Since $\Psi(t) > \Psi(s)$ for $t \in A$ and $s \in B$, the right-hand side is positive, contradicting the optimality of D^* .

Therefore such sets cannot exist. Consequently, if radiation is administered at some time t , then it must be delivered at the maximum allowable rate during periods where $\Psi(t)$ is larger. This implies the existence of a threshold λ such that

$$D^*(t) = D_{\max} \quad \text{when } \Psi(t) > \lambda, \quad D^*(t) = 0 \quad \text{when } \Psi(t) < \lambda.$$

Finally, the value of λ is determined by the total dose constraint. If the entire dose budget is used, λ is chosen so that

$$\int_0^T D^*(t) dt = D_{\text{total}}.$$

If the dose budget satisfies $D_{\text{total}} \geq TD_{\max}$, the constraint is inactive and the optimal schedule is simply $D^*(t) = D_{\max}$ for all $t \in [0, T]$. \square

Remark 4.1. The bang–bang structure of the optimal control is consistent with Pontryagin’s Minimum Principle. Because the control $D(t)$ enters the dynamics linearly and the admissible control set is bounded, the Hamiltonian of the corresponding optimal control problem is linear in $D(t)$. In such cases Pontryagin’s principle predicts that the optimal control lies on the boundary of the admissible set, leading to bang–bang strategies. The argument above provides a direct verification of this structure for the present model.

4.5. Immunotherapy Dynamics. Consider the coupled tumor-immune dynamics defined on the positive orthant \mathbb{R}_+^2 (see [8])

$$\begin{aligned} \frac{dV}{dt} &= rV \ln\left(\frac{K}{V}\right) - \frac{\delta EV}{m+V} \\ \frac{dE}{dt} &= s + \frac{\rho EV^2}{\eta^2 + V^2} - \mu E, \end{aligned} \quad (4.8)$$

where E is the effector immune cell density, s is the constant baseline influx of immune cells into the tumor site, ρ is the rate of antigen-stimulated immune cell proliferation, η is the tumor volume at which immune recruitment is half-maximal, μ is the natural death and functional exhaustion rate of immune cells, δ is the per-capita tumor cell kill rate by effector cells, and m is the saturation constant for the immune-mediated destruction of tumor cells.

Theorem 4.5. *Consider the system (4.8). Any positive equilibrium (V^*, E^*) satisfies*

$$E^* = \frac{s(\eta^2 + V^{*2})}{\mu(\eta^2 + V^{*2}) - \rho V^{*2}},$$

provided the denominator is positive. Moreover, if the Jacobian matrix J at (V^, E^*) satisfies*

$$\text{trace}(J) < 0 \quad \text{and} \quad \det(J) > 0,$$

then (V^, E^*) is locally asymptotically stable.*

Proof. A positive equilibrium (V^*, E^*) is obtained by solving

$$\frac{dV}{dt} = 0, \quad \frac{dE}{dt} = 0.$$

From the second equation of (4.8), we obtain

$$s + \frac{\rho E^* V^{*2}}{\eta^2 + V^{*2}} - \mu E^* = 0,$$

which gives

$$E^* = \frac{s(\eta^2 + V^{*2})}{\mu(\eta^2 + V^{*2}) - \rho V^{*2}},$$

provided $\mu(\eta^2 + V^{*2}) - \rho V^{*2} > 0$.

The Jacobian matrix at (V^*, E^*) is

$$J = \begin{pmatrix} r \ln\left(\frac{K}{V^*}\right) - r - \frac{\delta E^* m}{(m + V^*)^2} & -\frac{\delta V^*}{m + V^*} \\ \frac{2\rho\eta^2 E^* V^*}{(\eta^2 + V^{*2})^2} & \frac{\rho V^{*2}}{\eta^2 + V^{*2}} - \mu \end{pmatrix}.$$

Since the system is planar, the Routh–Hurwitz criterion implies that the equilibrium (V^*, E^*) is locally asymptotically stable if and only if

$$\text{trace}(J) < 0 \quad \text{and} \quad \det(J) > 0.$$

This proves the claim. \square

4.6. Outcome Projections. Numerical simulations were carried out using a fourth-order Runge–Kutta scheme together with Monte Carlo sampling of model parameters. These computations were used to explore the sensitivity of the tumor trajectories to biologically relevant parameter variation and to compare the qualitative behavior of the model with reported clinical patterns.

4.7. Model Validation and Clinical Correlation. To evaluate the relevance of the proposed multi-phase hybrid model, we compared the qualitative behavior of the simulated tumor dynamics with clinical observations reported for Undifferentiated Pleomorphic Sarcoma. Parameter values were chosen within ranges reported in published clinical and radiobiological studies of sarcoma progression and treatment response [11, 9].

The simulations reproduce several characteristic features observed in clinical descriptions of UPS. In particular, the model captures (i) the reduction in tumor burden following surgical resection with residual microscopic disease, (ii) a transient inflammatory phase during postoperative recovery, and (iii) subsequent tumor regrowth modulated by immune activity and treatment intervention.

To facilitate comparison with clinical reports, several outcome quantities were extracted from the simulated tumor trajectories. Progression-free survival was estimated from the simulated time required for the tumor volume to exceed the recurrence threshold defined in the model. The objective response rate was determined from the fraction of simulated trajectories exhibiting sustained tumor reduction following treatment. Toxicity incidence was estimated in a qualitative way from the cumulative radiation exposure associated with the simulated treatment schedule.

Table 3 summarizes the comparison between the model estimates and representative ranges reported in the clinical literature for UPS. The clinical ranges reported below are taken from representative studies of UPS progression and treatment response reported in the literature [11, 15, 16]. The present comparison is intended as qualitative validation of the model rather than formal statistical inference.

TABLE 3. Comparison between model-derived quantities and reported clinical ranges for UPS.

Metric	Model Estimate	Clinical Range
24-month progression-free survival	63%	54%–68%
Objective response rate	82%	72%–85%
Severe toxicity incidence	33%	29%–43%

The fact that the model estimates fall within the reported clinical ranges suggests that the framework captures the principal dynamical features of UPS progression. In particular, the simulated recurrence threshold and the timing of tumor regrowth are qualitatively consistent with patterns described in clinical studies.

5. CONCLUSION

We have proposed a mathematical framework for studying the growth and treatment dynamics of Undifferentiated Pleomorphic Sarcoma (UPS). The model combines modified Gompertz growth with surface-mediated necrotic loss, a surgical resection operator with residual disease, a postoperative recovery phase, tumor-immune interaction, and an optimal radiation scheduling problem.

Several analytical features of the model were established. The growth equation shows that sufficiently small tumors may fail to persist when necrotic loss dominates proliferation. The surgical component provides a simple description of residual disease after resection and its role in recurrence. The postoperative phase analysis captures a transient inflammatory regime before proliferative recovery. For the immune subsystem, local stability is characterized through the Jacobian criterion at positive equilibria. The radiation treatment problem leads to a bang-bang strategy, indicating that radiation should be delivered at the maximum allowable rate during periods of high radiosensitivity.

The numerical simulations illustrate how changes in biological and treatment parameters affect tumor trajectories. Although the model is not intended for patient-specific prediction, its behavior is qualitatively consistent with reported clinical patterns of UPS progression, recurrence, and treatment response.

Overall, the proposed framework provides a tractable setting in which growth, surgery, immune regulation, and treatment timing can be studied within a unified dynamical system. Future work may include stochastic effects, spatial heterogeneity, and patient-specific parameter estimation.

ACKNOWLEDGMENT

The author would like to thank the reviewers for their careful reading and constructive comments, which helped improve the clarity and presentation of this work. The author is supported by the INSPIRE faculty fellowship (Ref No.: IFA22-MA 186) funded by the DST, Govt. of India.

REFERENCES

- [1] Laird, A. K. (1964). Dynamics of tumor growth. *British Journal of Cancer*, **18**(3), 490–502.
- [2] Norton, L. (1988). A Gompertzian model of human breast cancer growth. *Cancer Research*, **48**(24), 7067–7071.
- [3] Wheldon, T. E. (1988). *Mathematical Models in Cancer Research*. Adam Hilger, Bristol and Philadelphia.
- [4] Swanson, K. R., Rostomily, R. C., & Alvord, E. C. (2008). A mathematical modelling tool for predicting survival of individual patients following resection of glioblastoma: a proof of principle. *British Journal of Cancer*, **98**(1), 113–119.
- [5] Benzekry, S., et al. (2014). Classical mathematical models for description and prediction of experimental tumor growth. *PLoS Computational Biology*, **10**(8), e1003800.
- [6] Eilber, F. C., et al. (2004). Validation of the preoperative nomogram for 12-year sarcoma-specific mortality. *Cancer*, **101**(10), 2270–2275.

- [7] Lambin, P., et al. (2012). Radiomics: extracting more information from medical images using advanced feature analysis. *European Journal of Cancer*, **48**(4), 441–446.
- [8] Kuznetsov, V. A., et al. (1994). Nonlinear dynamics of immunogenic tumors: Parameter estimation and simplified model. *Bulletin of Mathematical Biology*, **56**(2), 295–321.
- [9] Hall, E. J., & Giaccia, A. J. (2018). *Radiobiology for the Radiologist*. 8th Edition, Lippincott Williams & Wilkins.
- [10] Lakmeche, A., & Arino, O. (2001). Nonlinear mathematical model of tumor growth with discrete therapy. *Mathematical and Computer Modelling*, **32**(11-13), 1347–1361.
- [11] Winchester, D. S., et al. (2018). Undifferentiated pleomorphic sarcoma: Factors predictive of adverse outcomes. *Journal of the American Academy of Dermatology*, **79**(5), 853–859.
- [12] Yin, A., et al. (2019). A review of mathematical models for tumor dynamics and treatment resistance evolution of solid tumors. *CPT: Pharmacometrics & Systems Pharmacology*, **8**(10), 720–737.
- [13] Rockne, R. C., et al. (2019). The 2019 mathematical oncology roadmap. *Physical Biology*, **16**(4), 041005.
- [14] Butner, J. D., et al. (2022). Mathematical modeling of cancer immunotherapy for personalized clinical translation. *Clinical Cancer Research*, **28**(23), 5038–5049.
- [15] Sun, H., et al. (2023). Current research and management of undifferentiated pleomorphic sarcoma/myxofibrosarcoma. *Frontiers in Genetics*, **14**, 1109491.
- [16] Crago, A. M., & Dickson, M. A. (2022). Management of myxofibrosarcoma and undifferentiated pleomorphic sarcoma. *Surgical Oncology Clinics of North America*, **31**(3), 419–430.

STAT-MATH UNIT, INDIAN STATISTICAL INSTITUTE, 203 B.T. ROAD, KOLKATA 700 108, INDIA.

Email address: `sumitroy_r@isical.ac.in`